In-vehicle Monitoring Based on a Low-Cost mm-Wave Radar at 60 GHz

Antonio Lazaro
Electronics, Electrical and Automatics Eng. Dept.
Universitat Rovira i Virgili
Tarragona, Spain
antonioramon.lazaro@urv.cat

Nil Munte
Electronics, Electrical and Automatics Eng. Dept.
Universitat Rovira i Virgili
Tarragona, Spain
nil.munte@urv.cat

Ramon Villarino
Electronics, Electrical and Automatics Eng. Dept.
Universitat Rovira i Virgili
Tarragona, Spain
ramon.villarino@urv.cat

David Girbau
Electronics, Electrical and Automatics Eng. Dept.
Universitat Rovira i Virgili
Tarragona, Spain
david.girbau@urv.cat

***Abstract*—This work presents an in-vehicle monitoring system based on a PCR (Pulsed Coherent Radar) at the 60 GHz ISM unlicensed band. The radar can measure distances with sub-millimeter resolution. Therefore, a detection system has been designed for both seat occupancy and people's breathing monitoring since the radar has the capacity to measure displacements of the order of mm. The results of the respiration measurement agree with those obtained by another system whose measurements are based on the airflow, which allows its validation In addition, a proof-of-concept of gesture recognition based on the same radar is proposed.**

***Index Terms*—automotive radar, mm-wave radar, seat occupancy, detection, vital-sign monitoring, breathing monitoring, gesture recognition**

I. Introduction

Within the study areas associated with smart car technology, in-cabin monitoring of vehicles is becoming more frequent, as it implies improvements in aspects such as comfort and safety. The time that citizens spend on average per day driving is increasing due to the congestion in cities. Therefore, interest in the use of smart sensors that allow monitoring of the vital signs of the passengers and their physiological state has increased, In-cabin sensing based on radar technology is an emerging method to monitor the driver's health, emotions, and attention. Radar-based technology has advantages over cameras or optical sensors such as the capacity to detect objects through dielectrics and the preservation of privacy. Several applications have been proposed to improve safety and conform. Some of them are aimed at improving the human-machine interface using gesture recognition [1], passenger presence monitoring for airbag deployments [2], or vital sign monitoring for drowsiness detection [3]. This work studies the feasibility of using a low-cost pulse coherent radar (PCR) from Acconeer operating in the 60 GHz ISM unlicensed band for in-cabin applications. The radar is based on A111 radar sensor which is a System-in-Package (SiP) that integrates the mm-Wave front-end, the antenna, the memory, and the receiver in one chip. The radar is available in a low-cost (about 16 €) commercial module (XM132) ready for evaluation and integration. It transmits a modulated wavelet at the carrier frequency f_c=60 GHz, and can obtain the range to the target by measuring the delay between transmit and received pulses. It can measure with millimeter accuracy (typically 0.5 mm) between 60 - 2000 mm for an RCS of -21 dBsm. The signal-to-noise ratio (SNR) is improved by combining the signal from the transmission of phase-coherent pulses, resulting in better visibility of the object. The paper is an extension of a previous work [3] in which radar was used to monitor seat occupancy and occupant breathing. This work includes gesture recognition that can be used to control parameters such as air conditioning, audio volume, or opening of windows.

This work was supported by the Spanish Government grant PID2021-122399OB-I00 funded by MCIN/AEI/10.13039/501100011033, and by the EU's European Regional Development Fund (ERDF).

II. In-vehicle monitoring

A. Seat occupancy detection

In order to detect seat occupancy and breathing monitoring the radar is installed in front of the seat. In the event that the radar signal hits the body of a person inside the vehicle, the distance measured by the radar will be modulated caused by its breath which produces a periodic variation of the envelope of the received pulses [3]. The distance between the body and the radar can be modeled as the sum of the average distance r_0 and two terms that take into account the periodic movement of the chest, with maximum displacement r_b, and the random movements of the body induced by the car vibrations ($r_v(t)$):

$$r(t) = r_0 + r_b cos(2\pi f_b t) + r_v(t) \quad (1)$$

The radar firmware provides an envelope service that returns both the range and amplitude of the received envelope. Therefore, the delay of the peak of the envelope allows to estimate the distance to the body (r_0) and the fluctuations of

the peak amplitude give information about the movement and displacement of the chest due to breathing. When the seat is empty or occupied by an object, the radar detects the distance to the seat or object on the top of the seat (eg. a bag) meaning constant in time and its value is the same regardless of the instant in which it is measured. To estimate the presence of a person, the standard deviation of the AC component of the envelope amplitude is computed:

$$\sigma^2(t) = \int_0^t \left(\frac{dy}{dt}\right)^2 dt \tag{2}$$

A digital implementation of (2) is implemented with an exponentially weighted moving average (EWMA)from the samples of the measured peak amplitude $y[n]$ and the previous estimate of the standard deviation [3]. A simple fix threshold estimated from an empty seat is used to determine if the seat is occupied (see the block diagram of Fig. 1). An example of the operation of the seat occupancy indicator is shown in Fig. 2, in which the measurement begins with the engine off and the person occupying the driver's seat. After 30 seconds the driver gets out of the car and gets in after about 30 seconds. The driver starts the engine and after 50 seconds stops it and gets out of the car. It can be seen that both the range and the amplitude are almost constant when the seat is empty and the deviation is below the threshold even if the engine is on. When the presence of a person is detected the breathing algorithm described below determines their breathing rate (expressed in breaths by minute or bpm).

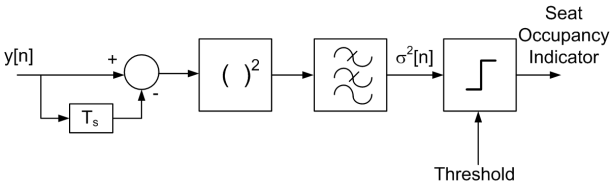

Fig. 1. Seat occupancy detector diagram [3]

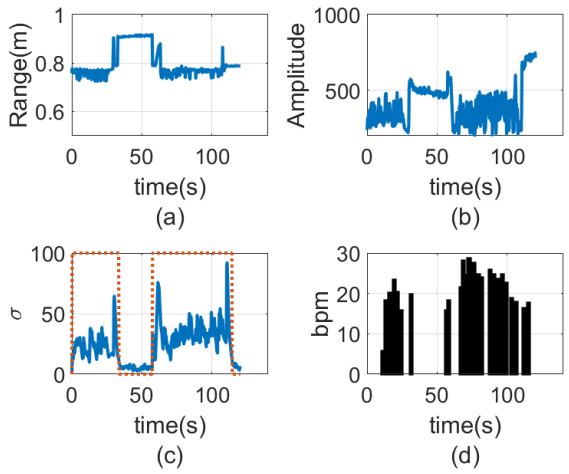

Fig. 2. Seat occupancy: (a) range, (b) amplitude, (c) deviation and seat occupancy indicator (dotted line), and (d) breathing rate [3]

B. Breathing monitoring

The breathing signal is obtained by applying a band pass filter between 0.1 Hz and 1 Hz to the amplitude of the envelope $y(t)$. To this end, a couple of filters are used, first a high pass-band filter to eliminate the DC component and then a low-pass filter that attenuates frequencies above 1 Hz to reduce noise. The filters are implemented using EWMA filters. The output of the filtered sequence $b[n]$ is used to determine the breathing rate from the time interval between two consecutive breaths. The peak detection algorithm proposed in [4] is used to detect the breaths. This method allows the detection of apneas (considered 10-second intervals without breathing) and breathing rate variability without the need for Fourier transform or other types of high computation signal processing that are more difficult to implement in real-time on low-cost microcontrollers. Additional details can be found in [3] and the block diagram is described in Fig. 3. The system has been tested in a real environment on a highway trip lasting one hour. Fig. 4 compares the breathing rate during the journey with that obtained by a reference air flow sensor located under the nose. The breathing rate is slightly lower and tends to be almost constant, which may indicate low driver activity and symptoms of a certain degree of drowsiness.

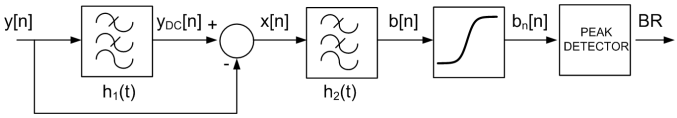

Fig. 3. Block diagram of the signal processing used to obtain the breathing rate [3].

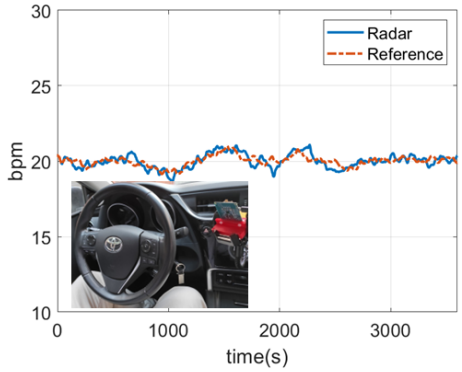

Fig. 4. Breathing rate as a function of time on a highway trip lasting one hour measured by the radar and the reference sensor (dashed line)

C. Gesture identification

This work explores the feasibility of identifying gestures from the time-range profile (peak envelope range as a function of time). Fig. 5 shows the time-range profiles for different gestures. Gestures that produce range changes have been chosen. For example, some of them have consisted in moving the hand up-down several times on the radar or from left to right or opening or closing the finger (clamp). To obtain data

for CNN training, the acquisitions are repeated 20 times for each gesture. Time range profiles are treated as back-white images. Half of the acquisitions have been used to train a convolution neuronal network (CNN) using Matlab toolbox, while the other half has been used to test. The CNN uses two internal convolution layers of 16 and 32 nodes, respectively. Bach normalization, a rectified linear activation function or reLU, and max pooling to down-sample are employed, and finally, a softmax function to connect the output layer. The accuracy obtained with the gesture set of Fig. 5 is 79%. The confusion matrix is shown in Fig. 6. It is observed that the errors increase with simpler gestures or that they are a subset of the others. Therefore, these classes can be removed. After that, the accuracy typically increases up to 90%. Using the trained neuronal network, each gesture is mapped to a command (eg. temperature air, volume, windows up/down, moving for the radio channel list, etc). After detecting the command, the range of the hand is used to increase or decrease the value in the same way as the analog slider bar. Figure 7 shows an example of moving the hand up and down as a function of time. To avoid false alarms, only the range of positions that falls within the radar observation window during a time interval is considered. In the case of not detecting any change in the movement of the hand after this period, the command is canceled. Although the number of independent gestures is not very high (5 to 7), when combined with the slider bar mode, it is possible to execute simple commands that improve man-machine communication avoiding distractions.

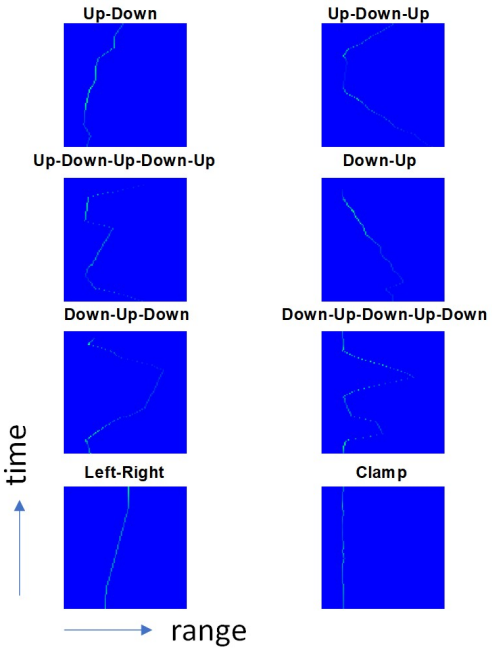

Fig. 5. Set of analyzed gestures

III. Conclusions

This work has explored the possibilities of an integrated pulse coherent Radar at 60 GHz ISM frequency band for

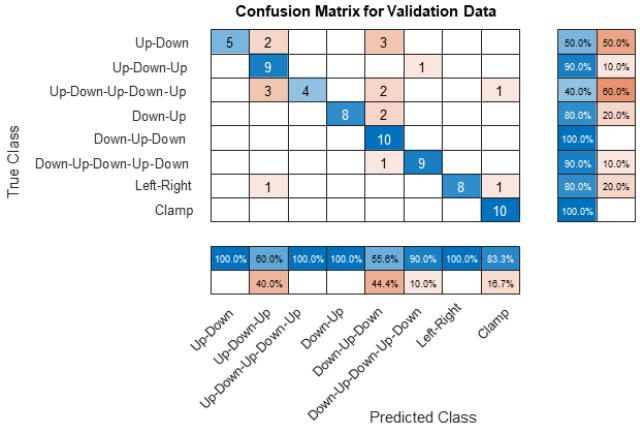

Fig. 6. Confusion matrix of the analyzed gestures

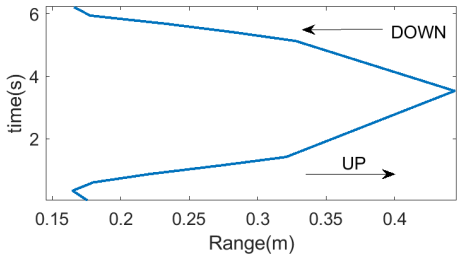

Fig. 7. Measured range of the path described by the hand once the start gesture is detected

in-vehicle applications. A seat occupancy detection system has been demonstrated. This system can detect the presence of people based on the standard deviation estimate of the peak amplitude differences. Together with the seat detector, it has been demonstrated from the fluctuations of the maximum amplitude of the signal that the breath rate can be obtained. The results obtained in real environments agree with those obtained using the air flow sensor The system can measure the breathing of the driver showing its potential use to monitor his state of drowsiness or fatigue. Some preliminary results have been presented for gesture recognition using the same radar from the time-range profiles to train CNNs. After recognizing the gesture, it is possible to use the measured range described by the movement of the hand as if it were a slide bar improving the human-machine interface, thus avoiding distractions.

References

[1] K. A. Smith, C. Csech, D. Murdoch, and G. Shaker, "Gesture recognition using mm-wave sensor for human-car interface," *IEEE sensors letters*, vol. 2, no. 2, pp. 1–4, 2018.

[2] N. Munte, A. Lazaro, R. Villarino, and D. Girbau, "Vehicle Occupancy Detector Based on FMCW mm-Wave Radar at 77 GHz," *IEEE Sensors Journal*, vol. 22, no. 24, pp. 24 504–24 515, 2022.

[3] A. Lazaro, M. Lazaro, R. Villarino, and D. Girbau, "Seat-occupancy detection system and breathing rate monitoring based on a low-cost mm-wave radar at 60 ghz," *IEEE Access*, vol. 9, pp. 115 403–115 414, 2021.

[4] S. Milici, A. Lázaro, R. Villarino, D. Girbau, and M. Magnarosa, "Wireless wearable magnetometer-based sensor for sleep quality monitoring," *IEEE Sensors Journal*, vol. 18, no. 5, pp. 2145–2152, 2018.